Accepted manuscript doi:
10.1680/jgein.24.00060

Accepted manuscript doi:
10.1680/jgein.24.00060

Submitted: 14 May 2024

Published online in 'accepted manuscript' format: 05 December 2024

Manuscript title: Milling of geosynthetic-reinforced asphalt layers: field operations and milling byproducts

Authors: Natalia S. Correia[1], Tiago R. Souza[1] and Jorge G. Zornberg[2]

Affiliations: [1]Federal University of Sao Carlos, Civil Engineering Department, Washington Luis Rd., km 235, Sao Carlos, Sao Paulo, 13.565-905, Brazil, [2]The University of Texas at Austin, Civil Engineering Department, University Station C1792 Austin, TX 78712-0280, USA

Corresponding author: Natalia S. Correia, Federal University of Sao Carlos, Civil Engineering Department, Washington Luis Rd., km 235, Sao Carlos, Sao Paulo, 13.565-905, Brazil

E-mail: ncorreia@ufscar.br

Accepted manuscript doi:
10.1680/jgein.24.00060

Abstract

With the increased use of geosynthetic interlayers, including geogrids, paving geocomposites and paving mats in asphalt rehabilitation works, an increase is also expected in projects involving the milling of asphalt layers that incorporate these geosynthetics. Although significant experience exists in milling conventional asphalt layers, such experience is limited when the milled material contains polymeric or fiberglass interlayers. Consequently, better understanding is needed on the differences in the milling process in asphalt layers with and without geosynthetics. In this study, an experimental field track was constructed at Salvador International Airport (Brazil), featuring five different geosynthetic-reinforced asphalt test sections that were milled after their construction. Evaluation of the field campaign results indicates that all geosynthetic interlayers proved to be “millable”. However, the milling operations exhibited varying milling efficiencies and resulted in milling byproducts (or Reclaimed Asphalt Pavement with Geosynthetics, G-RAP) with different physical characteristics. An average reduction of 18% in milling efficiency of reinforced asphalt layers was observed compared to that of unreinforced pavements. The G-RAP byproducts were found to include geosynthetic fragments of different sizes but mantained a particle size distribution similar to that of the control RAP. Furthermore, the collected G-RAP showed beneficial impact on mechanical characteristics of asphalt mixtures with 20% G-RAP, particularly in Marshall stability, flow, and indirect tensile strength, confirming their suitability for reuse in transportation applications.

Keywords: geosynthetics, asphalt rehabilitation, reinforced asphalt layers, milling, reclaimed asphalt pavement

Accepted manuscript doi:
10.1680/jgein.24.00060

Introduction

Regardless of the structure or durability of a flexible pavement, it will ultimately reach a stage in its service life when it needs rehabilitation, which often involves milling a portion of the preexisting asphalt layer and placing a new asphalt overlay. Rehabilitation programs produce significant amounts of asphalt byproducts, generally identified as “millings.” Due to the increased use of geosynthetic interlayers, such as geogrids, paving composites, and paving mats in asphalt rehabilitation works, the number of rehabilitation projects involving milling of asphalt layers that include geosynthetic interlayers has also been continuously increasing.

Asphalt millings, also known as Reclaimed Asphalt Pavement (RAP), have often been recycled, for example, by utilizing them as sources to produce new hot mix asphalt as unbound aggregates for construction of roadway bases or subbases, or as free-draining material in drainage systems, resulting in significant economic and environmental advantages. In summary, both the incorporation of geosynthetic interlayers and the recycling of pre-existing asphalt layers have become relevant sustainable practices. Yet, this has led to the need to properly assess the millability of geosynthetics within asphalt layers. According to Zaumanis et al. (2021), studying and improving milling parameters as a means of preparing a new constituent material is necessary, given that milling became an integral part of asphalt production. Properties of reclaimed asphalt pavement (RAP) are likely influenced by a variety of factors such as milling depth, speed of the milling equipment, drum rotational speed, pick layout, type of milling equipment and picks used, aggregate toughness, pavement type, age, and environmental conditions (West, 2015).

Accepted manuscript doi:
10.1680/jgein.24.00060

The integration of recycled asphalt and milled geosynthetic interlayers promotes sustainable construction practices and alternatives for the future of recyclable materials in roadway construction. Therefore, in addition to properly installing geosynthetics in overlay construction and benefiting from their well-stablized ability to reduce crack propagation, enhance pavement structural capacity, and minimize excess moisture (Correia and Zornberg, 2018; Canestrari et al, 2022; Kumar et al. 2023), understanding the milling process differences between geosynthetic-reinforced asphalt layers and conventional asphalt layers is crucial. Moreover, it is necessary to investigate the need of possible precautions during the milling process of geosynthetic-reinforced asphalt layers, with the reclaimed asphalt pavement (RAP) generated with geosynthetic fragments, referred to herein as G-RAP, emerging as a potentially new recyclable material.

The existing literature on milling of asphalt-reinforced layers is limited, with further challenges posed by the wide range of available reinforcement products. These include polymeric, fiberglass, and carbon or basalt products, each with distinc tensile properties, mesh openings, and additional features such as ultra-thin fabric or geotextile backing, including geosynthetics that are self-adhesive or bitumen-coated (Correia et al. 2024). Very few studies specifically address the milling of geosynthetic-reinforced asphalt layers, and no comparative studies have been conducted between products with differing characteristics. Damisch and Kirschner (1994), pioneers on this topic, built a polymeric geosynthetic-reinforced full-scale test track, which was subjected to milling processes by varying the milling equipment rotation speed and wetting. Despite disruptions reported in the milling process, they concluded that

geosynthetic-reinforced pavement was millable. Research by Tran et al. (2012), Gu et al. (2021), Nguyen et al. (2021) evaluated the mechanical properties of RAP originated from milled fiberglass reinforced asphalt layers, although no assessment was made of differences in the milling process or the degree of millability of different products. Saxena et al. (2023) found that the presence of a nonwoven geotextile does not affect the millability of asphalt layers. However, designers and roadway agencies are often questioning the ability of geosynthetics to produce fiber fragments, or to interfere with the milling process at the time of deciding on the use of geosynthetics in a rehabilitation program.

One of the possible recycling strategies involving the use of G-RAP is its use in the production of fresh asphalt mixtures. Damish and Kirschiner (1994) investigation on this topic reported an increase in Marshall stability in mixtures containing G-RAP. In contrast, Tran et al. (2012) noted minimal differences in strength between mixtures containing RAP and G-RAP, suggesting that the presence of geosynthetics does not significantly alter the properties of the final asphalt mixture. Nguyen et al. (2021) conducted laboratory studies and indicated no difficulty in reusing RAP containing 30% glass grid residues in the selected asphalt mix, and suggests that results will depend on the quality of the milling.

In the present study, full-scale pavement sections with geosynthetic-reinforced asphalt layers were milled at the Salvador International Airport, Brazil. The sections had been constructed using paving geosynthetics with different physical and mechanical properties. The effectiveness of the milling process of sections involving geosynthetic interlayers was compared with that of a conventional unreinforced pavement section using milling practices employed in

airport operations. This study assesses the viability of milling operations and proposes new indicators of milling efficiency. In addition, the G-RAP byproducts resulting from the milling of the different test sections are characterized in order to assess potential differences in physical parameters that will be relevant in the selection of potential recycling strategies. The findings of this study can provide valuable insight into the milling process of geosynthetic-reinforced asphalt overlays and emphasize the importance of further research to fully understand the implications of geosynthetic interlayer type on milling efficiency.

2 Overview of the full-scale field program

2.1 Full-scale experimental test sections

Full-scale field test sections were constructed in this study at Salvador International Airport, Brazil. Operated by the Vinci Group, the 'Luíz Eduardo Magalhães' Salvador International Airport is located approximately 30 km from "*Bahia de Todos os Santos"* in Salvador, Bahia, Brazil. With an average of 91 daily flight operations, the airport serves approximately 6.8 million passengers annually.

The test sections were constructed near aircraft Parking Area 3, in a location with no aircraft or vehicle traffic, which provided comparatively better control over the test sections. The original paved structure consisted of a clayey silt subgrade, a 180-mm-thick aggregate base, and a 60-mm-thick asphalt layer with an aggregate nominal size of 12.7 mm. The testing area was selected in order to avoid presenting cracks, potholes, and joints. The test sections included an unreinforced (control) section and five geosynthetic-reinforced sections, as indicated in Figure 1. The following steps were executed to achieve proper surface preparation, tack coat application,

geosynthetics placement, asphalt overlay construction, and milling operations. This section briefly explains each of these steps.

Step 1: Surface Preparation

The original pavement structure initially underwent a milling process to simulate the actual conditions of a rehabilitation project before the installation of the geosynthetic interlayers and placement of a new asphalt overlay. Specifically, this stage involved milling the top 20 mm of the old asphalt layer using a Wirtgen W1000L milling machine, leaving the remaining bituminous layer at a thickness of 40 mm, with grooves averaging 1.2 mm in depth. Figure 2 illustrates the milling process and the surface texture prior to geosynthetics installation.

Step 2: Tack Coat Application

The tack coat application was conducted following the surface preparation. The tack coat material and application rate are typically product-specific. Asphalt emulsions are predominantly used as tack coat in South America, particularly for pavement construction and maintenance. The approach used in the present research focuses on the milling aspects of the process for different geosynthetics, without considering different combinations of binder types or tack coat rates. Accordingly, all geosynthetics evaluated in this study were installed using the same asphalt emulsion content, selected based on the practice established by the Airport operator.

For the tack coat application, the pavement surface was required to be dry and clean. After cleaning the area, a cationic rapid setting asphalt emulsion type 2 (CRS-2), was applied to all test sections at an average rate of 660 g/m^2 (residual) according to standard practice at Salvador International Airport. The CRS-2 emulsion has a Saybolt Furol viscosity at 50 °C

(ASTM 7496, 2018) of 182.5 s, a penetration (0.84 mm) of 0.03% mass (ASTM 6933, 2018), and a residual binder content of 53% (ASTM 6997, 2020). The emulsion was uniformly applied using a spray bar at a temperature set to 55°C. The ack coat curing time was set as 30 minutes. Figure 3 illustrates the tack coat application process.

Step 3: Geosynthetic installation

The geosynthetic interlayers used in this investigation included a high-modulus fiberglass geogrid with a polymeric coating (GS1), a geocomposite reinforcement involving a fiberglass geogrid attached to a polypropylene (PP) geotextile fabric backing (GS2), a micro fiberglass mesh embedded into high polyester (PET) mat (GS-3), a geocomposite reinforcement comprising a fiberglass geogrid attached to a PP ultralight fabric backing (GS4), and a geocomposite reinforcement comprising a PET geogrid attached to a PP ultralight fabric backing (GS5). These products are commonly used geosynthetic types for asphalt applications and are expected to provide a reinforcement function within the asphalt layers via a tension development mechanism. It should be noted that installation of the geosynthetics took place during the Pandemic, which posed additional logistical and operational challenges. These circumstances limited the number of geosynthetic materials adopted in the study. Figure 4 shows the various geosynthetic interlayer used in this study, while Table 1 presents their main characteristics.

After emulsion break, the different geosynthetic interlayers were installed in the test sections manually by the airport pavement crew, avoiding wrinkles and folds. All geogrid composites were installed with geogrid side facing up. Although some fiberglass geosynthetic interlayers have been typically installed on a leveled asphalt surface, in the present study, in

order to avoid influencing factor in the milling process, all the geosynthetic interlayers were directly installed over the milled surface according to airport practices. While it is recognized that the GS2 product, due to its high asphalt retention capacity (Table 1), may require a comparatively greater tack coat rate for optimal shear bond performance, the same tack coat rate was adopted for all test sections, which facilitated comparison of millability operations among different products. For example, adopting high binder rates could have led to bleeding in some of the sections with other geosynthetic interlayers.

In the present study, overlaps were not necessary during geosynthetics installation; however, when necessary, they should be performed between 50 mm to 150 mm, with consultation with the manufacturer. Figure 5 presents the geosynthetic interlayer installation in the experimental test sections.

Step 3: Asphalt overlay construction

Figure 6 presents asphalt overlay construction. To prevent significant wrinkles caused by the paver wheels over the geosynthetic, the adopted solution involved lightly spreading hot mix asphalt from the paver hopper along the wheel paths (Figure 6a). This procedure, referred to as *asphalt sanding technique* is also recommended by Kumar et al. (2023). In the present research, no adverse effects from the tack coat due to the tracking of construction equipment wheels were observed during installation. The asphalt concrete overlay was subsequently compacted (Figure 6b), an operation that involved placing a 60-mm-thick layer composed of crushed limestone aggregates (maximum nominal size of 12.7 mm) and binder type PG 58-16 at an optimum bitumen content of 4.66% by aggregate weight. The temperature of the hot mix asphalt

application was set to 120°C. Additonal details on the construction process can be found in Correia et al. (2023). Final test section, illustrating the direction of milling direction is shown in Figure 6d.

2.2. Milling operation and collection of G-RAP

To identify possible differences in the milling process among the different sections (geosynthetic-reinforced sections and the control section), the milling machine, movement speed, and drum rotational speed remained unchanged throughout field operations to minimize the possible influence of such milling parameters.

In this study, a Wirtgen W1000L milling machine was used, as it is commonly employed in maintenance work at Salvador International Airport. The machine is equipped with a standard milling drum containing 92 milling picks and has a total milling width of 1000 mm. In this configuration, it can mill conventional asphalt layers at its maximum speed of 320 rpm. The distance between milling picks is 180 mm. Figure 7 provides details of the milling machine and the picks with cap-shaped carbide tips used in this study. Since the equipment was provided by the airport operator , it was not possible to modify the number of variables in the milling process (e.g. equipment type, rotational speed, cutting width and cutting depth) to explore the impact of milling parameters on the efficiency of the milling process and the quality of the produced G-RAP.

The execution of the milling operations were carefully planned to ensure that the simulation closely resembled an actual asphalt rehabilitation process. To prevent premature wear of milling picks and to ensure proper milling, it is common for milling equipment to incorporate

a water spraying device on the milling drum. This device was also referenced in the study by Damisch and Kirschner (1994), where the authors reported turning off the water spray during milling at a certain point. In the present study, continuous water spraying was maintained throughout the operations, as is typically done in field. A small section outside the test area was milled, leading to the calibration of the water-spraying device to ensure sufficient cooling without pooling in the milled region. Preliminary tests on the milling machine revealed that the water volume was initially higher than necessary, which resulted in the adoption of a milling depth of at least 25 mm below the geosynthetic elevation.

The milling process in both the geosynthetic-reinforced and control sections was carried out at a constant maximum milling drum speed of 320 rpm. The same machine operator performed the milling operations consecutively across all six test sections. The cutting depth was set at 90 mm, which is 30 mm below the geosynthetic interlayer positioned between the new and old asphalt layers. The milling was performed longitudinally along the 10-meter-long experimental test sections. Before starting the field program, all milling picks were replaced to ensure proper milling of the asphalt material. Figure 8 presents the cross-sections for the different phases of the present study.

The milling time for each field test section was recorded, along with observations of any obstacles encountered during the milling process. Both the G-RAP and control RAP were collected by dump trucks, which were loaded via the milling machine’s conveyor belt. The collected materials were stored in designated bays within a covered area at the airport. Figure 9

shows the milling equipment and details of the geosynthetic interlayer between the asphalt layers.

To minimize the impact of pick wear on the millability results, the milling picks were replaced at the start of operations in each section. The machine's travel time for each 10.0-meter-long section was monitored with a stopwatch, and the target drum rotation during the milling process was observed for each section. The control section was milled first, followed by sections GS1, GS2, GS3, GS4 and GS5.

The millability of the various test sections reinforced with paving geosynthetics was evaluated both visually during the milling operations and subsequently using the collected videos and photos. This evaluation included documenting any difficulties encountered during the milling process, as well as quantifying the potential tangling of geosynthetic fragments around the drum during and after the milling operation. The observation and note-taking process was systematically carried out for the different reinforced sections to enable a proper comparison among the different test sections.

3. Milling efficiency of geosynthetic-reinforced asphalt layers

Milling of the control section proceeded as expected for milling operations, with no disruptions in the process, and the milling time remained within the expected range for a W1000L machine. Specifically, the total milling time in this case was 96 seconds for a 10-meters-length and a milling depth of 90 mm, resulting in a speed of 6.25 m/min. This milling time was adopted as a baseline for comparison with other sections to assess the milling

efficiency of geosynthetic-reinforced sections. The resulting control RAP (RAP-C) was collected and stored in a covered area at the airport yard.

Initial observations of the milling processes for the fiberglass products (GS1, GS2, GS3, and GS4) generally indicated no disruptions in the process, with millability considered equivalent to that of a control (unreinforced) asphalt layer. No geosynthetic fragments or filaments were observed to become entangled in the milling drum at the end of the milling processes of for the various fiberglass-reinforced asphalt sections (GS1, GS2, GS3 and GS4). Figure 10 shows representative stages during the milling process of the fiberglass products. The completed milling of the fiberglass-reinforced asphalt sections can be seen in Figure 10a, while a view of the milling drum (after milling these geosynthetic sections) is shown in Figure 10b. Observations made during the milling process, as well as through photos and videos, revealed the presence of geosynthetic fragments in the material transfer from the conveyor belt to the truck's collection drum (Figure 10c), along with some larger fiber fragments of GS1 that were easily noticeable in the G-RAP produced (Figure 10d). The G-RAP2, which involved a comparably thick geotextile backing, showed similar characteristics to G-RAP-1, although with somewhat larger aggregate millings and some visible geotextile fragments (Figure 10e).

The millings resulting from the section with G-RAP3, composed of a thin fiberglass mat, resembled the RAP-C milling, with slightly larger aggregates and some visible fragments of the fiberglass mat. The G-RAP4, which contains a fiberglass geogrid with an ultralight geotextile backing, exhibited the typical appearance of RAP-C, with small fiberglass fragments (fiber size) and visible fiberglass dust.

Accepted manuscript doi:
10.1680/jgein.24.00060

For the section reinforced with GS5, a product manufactured with a polyester geogrid with an ultralight geotextile backing, no disruptions were noted in the milling process along the 10-meter track, similar to the process described for the fiberglass products. However, at the end of the milling operation of the GS5 section, some geogrid filaments were found to become entangled in the milling drum. Nonetheless, these entangled fragments did not disrupt the continuity of the milling process along the length of the section and could be easily removed from the drum. Also, it was not necessary to cut the geosynthetic fragments, but only to uncoil them from the drum. The collected polyester filaments were then stretched on-site for length measurement and weighing. Figure 11 depicts the milling process of the polymeric-reinforced asphalt section.

The occurrence of tangled geogrid in the milling drum corroborates the reports of milling geosynthetic-reinforced asphalt sections by Damish and Kirschiner (1994), who reported that milling speed had to be reduced to uncoil polyester geogrid filaments from the milling drum. The results observed by Damisch and Kirschner (1994) reported lengths of the collected polyester filaments reached a maximum of 300 mm. Instead, the lengths of polyester filaments collected from the milling drum in this study ranged from 90 mm to 128 mm. Overall, in the present study, the 90-mm-deep asphalt layers containing geosynthetic interlayers were successfully milled, showing no significant differences compared to milling a control section, except from the observed presence of the geosynthetic fragments in the GS5 section.

To quantify the percentage of polyester fragments (GS5) in the milling drum at the end of the milling process, the entangled material (Figure 11b) was weighed in the laboratory. The

observed mass was compared to the mass per unit area of the geosynthetic installed in the filed section (Table 1). The fraction of material tangled in the milling drum (115,0 g) compared to the total mass of geosynthetic present in the test section (2448,0 g) was determined to be 4.7%, which was deemed to be small. It should be noted that the test section constructed as part of this study, measuring 10-meters-length, is relatively small. In larger projects, this issue could lead to operational challenges, such as machinery malfunctions or reduced milling quality. Therefore, it highlights the need for awareness and possibly preventive measures when conducting milling services on a larger scale.

Table 2 details the total milling time recorded for each section, the moving speed of the milling machine, and the milling efficiency of the sections with geosynthetics compared with the control section. The results presented in Table 2 indicate the differences in milling time based on the type of geosynthetic used in the asphalt overlays compared to the control section. In the section with product GS1, the milling process took 99.0 seconds, which is only slightly longer than in the control section (96.0 seconds), suggesting virtually no additional resistance to the milling process. In the case of GS2, the milling time was recorded as 117.0 seconds, indicating a slight increase in milling resistance, possibly due to the combination of materials in the geocomposite structure (nonwoven geotextile + fiberglass geogrid). In the case of the section reinforced with GS4, the milling time was similar to that of GS2, taking 118.0 seconds, possibly also because the product involves a combination of materials in the geocomposite structure. In contrast, the "Paving mat" (GS3), an ultrafine fiberglass micro fiberglass mesh, exhibited a slight reduction in milling time (114.0 seconds) compared to the previous geocomposites, suggesting

Accepted manuscript doi:
10.1680/jgein.24.00060

only a comparatively small additional resistance to milling relative to the control section. The GS5 geocomposite (polyester) exhibited the longest milling time at 145.0 seconds, indicating comparatively higher resistance compared to the other tested geosynthetic interlayers.

Overall, all milling times for the sections involving geosynthetic reinforcement were longer than that of the control section, with an efficiency that is, in average, 18% slower relative to the baseline milling time. This indicates the development of resistance to the cutting process due to the presence of geosynthetic reinforcement within the asphalt layers. Among the tested products, the polyester geocomposite showed the longest milling time, followed by those containing nonwoven geotextiles in their structure.

It is important to highlight that the recorded efficiencies depend on the milling equipment used in the present study. Milling machines with higher rotation speed are expected to achieve enhanced efficiencies in geosynthetic-reinforced asphalt layers. While this study focuses on the efficiency of the milling process of asphalt layers including geosynthetic interlayers, it should be acknowledged that different geosynthetics and other characteristics of the overlay and milling processes parameters (e.g. tack coat rate, tack coat type, milling surface conditions, milling equipment, milling depth), may influence milling efficiency

4 Characteristics of the G-RAP

The G-RAP stockpiles at the airport were evaluated to determine the presence of geosynthetic fragments in the produced RAP, along with milled materials of varying sizes. As antecipated, filaments and geosynthetic particles were identified in the G-RAP stockpiles. Notable differences in the sizes of fiber, milled geotextile fragments, and fiberglass powder presence were observed

among the stockpiles of the different G-RAP materials. Figure 12 illustrates the G-RAP storage area, stockpiles and aspects of the different collected G-RAP.

As illustrated in Figure 12c, the reclaimed asphalt pavement with Geosynthetic 1 (G-RAP1, with a fiberglass geogrid), exhibited an overall appearance similar to that of the control asphalt milled material, although with noticeable presence of isolated fiberglass filaments. G-RAP2 displayed characteristics of a coarser milling, with isolated fragments of geotextile and short fiberglass geogrid filaments. The G-RAP3, involving a relatively thin geocomposite made of fiberglass mesh, showed an appearance similar to a typical RAP milling of coarser gradation, although containing only comparatively few fragments of the fiberglass mesh. The G-RAP4, involving a geocomposite consisting of a fiberglass geogrid and ultralight geotextile, showed the appearance of a finer RAP milling, with small fragments of fiberglass (visible as short fibers) and a visible presence of fiberglass powder. Lastly, the G-RAP5, which involves a polyester geocomposite (visible as short fibers), exhibited an appearance similar to the aggregates of the control RAP, with smaller polyester fibers. Specifically, in the case of GS5, despite showing tangled geogrid polyester filaments in the milling drum, G-RAP5 exhibited smaller and less noticeable geosynthetic fragments compared to those from geogrid GS1 and other geocomposites.

The visual assessment implies that there are differences among G-RAP samples, particularly in terms of particle size and the characteristics associated with the presence of each milled geosynthetic fragments. In the cases of G-RAP2 and G-RAP3, geotextile fragments were visually identifiable. Such a presence was also reported by Saxena et al. (2023).

Accepted manuscript doi:
10.1680/jgein.24.00060

In order to quantify the differences among the various G-RAP, samples were further evaluated at the Geosynthetics Laboratory at the Federal University of Sao Carlos. Figure 13 shows the particle size distribution curves of the different G-RAP collected in the present study. The results in this figure indicate that there were no significant differences among the particle size distribution curves of RAP-C and different G-RAP samples. Even among the G-RAP samples, the particle size distributions are reasonably similar, with larger aggregates in GRAP-1 and GRAP-2. This supports the previous observation that asphalt overlays reinforced with different geosynthetics, when compared to conventional asphalt overlays, produce milled materials that can be reused in applications similar to those for conventional RAP.

The fragments of geosynthetics were found to vary in size depending on the G-RAP samples, depending on the specific geosynthetic components. In this study, a significant effort was made to quantify geosynthetic particle sizes. Yet, retrieving the geosynthetic fragments within the RAP samples was unfeasible. Figure 14 shows G-RAP particles retained in sieve #200. Overall, among fractions of fibers, a comparatively significant number of fibers was visible for sizes ranging from 2 to 10 mm, although a significant fraction of finer particles were also observed.

To quantify the total mass of geosynthetics expected to be present in the G-RAP samples, the mass of the as-intalled geosynthetic products was calculated. This calculation enables the determination of the expected mass fraction of geosynthetics installed relative to the mass of the asphalt mixture. Considering the experimental track section used in the present study, for an area that 1 meter square and 90 mm thick (milling depth), with an asphalt mixture density of 2,433 kg/m^3, the total mass of RAP is approximately 219 kg/m^2. The fraction of geosynthetics

Accepted manuscript doi:
10.1680/jgein.24.00060

fragments anticipated in the G-RAP samples is therefore 1.88 g/kg in G-RAP1, 1.74 g/kg in G-RAP2, 0.66 g/kg in G-RAP3, 1.49 g/kg in G-RAP4, and 1.24 g/kg in G-RAP5. This result represents geosynthetic fiber content (by weight of aggregates) of 0.19% (G-RAP1), 0.17% (G-RAP2), 0.07% (G-RAP3), 0.15% (G-RAP4) and 0.12% (G-RAP12), based on the 90 mm depth milled asphalt layer considered in this stdy. The calculated fraction of geosynthetic fragments is notably higher than the fraction of 'visible' geosynthetic fragments in the retrieved samples.

The aim of this research is to assess the millability of different geosynthetics and quantify physical characteristics of the resulting byproducts (G-RAP). However, the suitability of these characteristics will depend on the intended reuse of G-RAP (e.g. to produce new asphalt mixtures, for use as base or subbase courses, for use as aggregate in drainage layers). Overall, results presented herein show that there was no significant differences between the aggregate millings of the produced G-RAP samples in comparison with control RAP, apart from the presence of geosynthetic fragments. To the authors' knowledge, this investigation possibly represents the first comprehensive study on milling of geosynthetic-reinforced asphalt layers and the resulting byproducts. .

5. Reuse of G-RAP for production of new asphalt mixes

The physical characterization of G-RAP discussed in the previous section is relevant for different recycling strategies. Among them, G-RAP may be considered for reuse to produce recycled asphalt mixes. In this case, additional characterization is necessary, which typically includes an assessment of the rheological properties, binder content, and gradation of the RAP. Furthermore, necessary tests may include the use of rejuvenators or recycling agents to reduce

the viscosity of the aged and hardened bitumen, ensuring the mixes meet the required specifications for durability.

As a preliminary evaluation of milling byproducts to produce recycled asphalt mixes, the Marshall stability and flow tests (ASTM D6927-15), as well as indirect tensile tests (ASTM D6931-17), were conducted as part of this study. In particular, 20% RAP-C and 20% G-RAP samples were used to prepare recycled hot asphalt mix samples with maximum aggregate size of 1 in. (19 mm), which is consistent with Technical Standard 031/2024 of the Brazilian Department of Transportation (DNIT, 2024). Table 3 presents the results of this testing program. As observed in this table, no significant performance differences can be observed in the results obtained using recycled material samples with and without geosynthetic fibers and the reference mix. The optimum bitumen content observed for the mixtures with 20% G-RAP ranged from 5.2% to 5.5%, while RAP-C reached optimal parameters at an optimum bitumen content of 5.6%. This indicates that recycling RAP from geosynthetic-reinforced pavements is expected to behave no differently than using conventional RAP. The results show a trend in reducing the amount of binder needed for new asphalt mixtures containing geosynthetic fragments.

Regarding the stability tests, flow, and indirect tensile test, all the recycled asphalt mixtures containing 20% G-RAP showed results above the minimum design specification, also indicated in Table 3. These results show not detrimental influence of the geosynthetic fibers and fragments on the mechanical parameters of the asphalt mixture, which, in some cases, yielded results superior to those of the mixture recycled with 20% RAP-C, especially in terms of flow and indirect tensile strength.

Accepted manuscript doi:
10.1680/jgein.24.00060

The findings from this research show that asphalt layers with paving geosynthetics (both fiberglass and polyester) can be successfully milled and the G-RAP samples produced show characteristics that makes them suitable for reuse in various recycling strategies (e.g. asphalt mix, base course, drainage layers). The actual implementation of the results into such production requires additional evaluations, which are beyond the scope of this study. The results generated as part of this study also support the viability of using G-RAP to specifically produce recycled asphalt mixtures, reinforcing the potential for sustainable practices in pavement rehabilitation. Future studies are recommended to investigate which specific milling parameters most influence the properties of milled G-RAP. Such investigations will enhance the understanding of G-RAP's behavior and performance in recycled asphalt mixes, leading to improved recycling strategies.

4. Conclusions

This study examined the milling process of geosynthetic-reinforced asphalt overlays, focusing on its feasibility and the potential potential impact of the presence of geosynthetics on asphalt milling efficiency. In addition, the study evaluated the physical characteristics of the milling byproducts, as well as additional characteristics relevant to cases in which the millings are reused for the production of recycled asphalt mixes. The following conclusions can be drawn from the present study:

- Flexible pavementsthat have been rehabilitated with geosynthetic-reinforced asphalt overlays can be successfully milled. Specifically, the presence of geosynthetic reinforcements was found not to result in significant disruptions of milling operations. Specifically, the asphalt layers in this study could be milled entirely using a W1000L

machine and maintaining other parameters constant (e.g., drum rotational speed, movement speed). Continuous water spraying during milling was found to facilitate the operations.

- The milling operations of geosynthetic-reinforced sections (GS1 to GS5) showed comparable or slightly extended milling times to that of the control section, indicating only minor additional resistance due to the presence of fiberglass or polyester inclusions. Despite a slight increase in milling time for the polyester geogrid section, the operations are deemed acceptable.
- The evaluation of G-RAP samples revealed the visible presence of geosynthetic fragments within the millings. The visual appearance and measured characteristics of G-RAP were influenced by the type of geosynthetic. However, the G-RAP particle size distribution was essentially independent of the type of geosynthetic material, remaining similar to that of the control RAP.
- Based on the mass of the as-installed geosynthetic products, the fiber content ranged from 0.07% to 0.19% by weight of the aggregate, considering a milling depth of 90 mm. However, the fiber content actually identified in the G-RAP was smaller, since geosynthetic fragments were often indistinguishable from the rest of the milled mass. Among the fibers visible within G-RAP samples, a significant fraction was found to range in length from 2 to 10 mm.
- Asphalt mixes incorporating 20% G-RAP were found to perform comparably to control mixes with 20% RAP, based on the results of Marshall stability, flow, and indirect tensile

strength tests. Furthermore, the observed optimum bitumen content for G-RAP mixtures aligned closely with that of conventional RAP, suggesting the feasibility of adopting G-RAP in different recycling strategies. In particular, the results of Marshall stability, flow, and indirect tensile strength tests for all recycled mixtures met or exceeded minimum design specifications.

The field and experimental components of this study were conducted using several geosynthetic types, but they constitute only a fraction of the geosynthetic interlayers available for asphalt overlays. In addition, the results correspond to overlays placed using a specific tack coat type and application rate and to milling operations conducted with specific equipment. Extrapolation of the results beyond the range of parameters adopted in the present study should be conducted with caution.

Credit authorship contribution statement

Natalia S. Correia: Conceptualization, Supervision, Investigation, project administration, writing original draft, writing – review & editing.

Tiago R. Souza: Investigation, Methodology, formal analysis, writing original draft.

Jorge Zornberg: Investigation, writing – review & editing.

Acknowledgement

The authors thank the support received from Vinci Airports Group, International Airport of Salvador, SOLOCAP Geotecnologia, Pavitec Engineering and the Laboratory of Geosynthetics of the Federal University of Sao Carlos.

Accepted manuscript doi:
10.1680/jgein.24.00060

Declaration of Competing Interest

The authors have no conflicts of interest to declare that are relevant to the content of this article.

Data availability statement

The data that support the findings of this study are available from the corresponding author upon reasonable request.

Accepted manuscript doi:
10.1680/jgein.24.00060

Abbreviations

CRS-2 - cationic rapid setting asphalt emulsion type 2

G-RAP - Reclaimed Asphalt Pavement with Geosynthetics

G-RAP1 - Reclaimed Asphalt Pavement with Geosynthetic 1

G-RAP2 - Reclaimed Asphalt Pavement with Geosynthetic 2

G-RAP3 - Reclaimed Asphalt Pavement with Geosynthetic 3

G-RAP4 - Reclaimed Asphalt Pavement with Geosynthetic 4

G-RAP5 - Reclaimed Asphalt Pavement with Geosynthetic 5

GS1 – Geosynthetic 1

GS2 – Geosynthetic 2

GS3 – Geosynthetic 3

GS4 – Geosynthetic 4

GS5 – Geosynthetic 5

PET – Polyester

PG – penetration grade

PP - Polypropylene

RAP - Reclaimed Asphalt Pavement

RAP-C - control RAP

Rpm – rotation per minute

References

ASTM (2020) D 6637: Standard Test Method for Determining Tensile Properties of Geogrids by the Single or Multi-Rib Tensile Method. ASTM International, West Conshohocken, PA.

ASTM (2018) D5261: Standard Test Method for Measuring Mass per Unit Area of Geotextiles. ASTM International, West Conshohocken, PA.

ASTM (2022) D6140: Standard Test Method to Determine Asphalt Retention of Paving Fabrics Used in Asphalt Paving for Full-Width Applications. ASTM International, West Conshohocken, PA.

ASTM (2015) D6927: Standard Test Method for Marshall Stability and Flow of Asphalt Mixtures. ASTM International, West Conshohocken, PA.

ASTM (2017). ASTM D6931-17: Standard Test Method for Indirect Tensile (IDT) Strength of Asphalt Mixtures. ASTM International, West Conshohocken, PA.

Brazilian Department of Transport (2024). Technical Standard DNIT 031/2024 – ES: Specifications for asphalt mixtures. DNIT. Brasilia, Brazil.

Canestrari F, Cardone F, Gaudenzi E, Chiola D, Gasbarro N, Ferrotti G (2022) Interlayer bonding characterization of interfaces reinforced with geocomposites in field applications, Geotext. Geomembranes, **(50)**, pp. 154-162.

Correia NS, Zornberg, JG (2018) Strain distribution along geogrid-reinforced asphalt overlays under traffic loading, Geotextiles and Geomembranes, (46), Issue 1, Pages 111-120.

Correia NS, Souza TR, Silva MPS, Kumar VV (2023) Investigations on interlayer shear strength characteristics of geosynthetic-reinforced asphalt overlay sections at Salvador International Airport, Road Mater. Pavement Des., **24 (6)**: 1542–1558.

Correia NS, Silva MPS, Shahkolahi A. (2024) Optimum tack coat rate for different asphalt geosynthetic interlayers to achieve optimum shear bond strength, Geotextiles and Geomembranes, (52), Issue 4, Pages 778-789.

Damisch A and Kirschner R (1994) Recycling of Grid Reinforced Asphalt Pavements. In *Proceedings of the Fifth Intern. Conference on Geotextiles, Geomembranes and Rel. Products*, 105–108 (1994).

Gu F, Andrews D, Marienfeld M. (2021) Evaluation of Bond Strength, Permeability & Recyclability of Geosynthetic Products. In *Proceedings of the Geosynthetics Conference* (Melissa Beauregard Jennifer E Nicks), Online, p 362.

Kumar VV, Roodi GH, Subramanian S, Zornberg JG (2023) Installation of geosynthetic interlayers during overlay construction: Case study of Texas State Highway 21, Transportation Geotechnics, **(43)**: 101127

Nguyen ML, Hornych P, Le XQ, Dauvergne M, Lumière L, Chazallon C, Sahli Mehdi, Mouhoubi S, Doligez D, Godard E (2021) Development of a rational design procedure based on fatigue characterisation and environmental evaluations of asphalt pavement reinforced with glass fibre grid, Road Materials and Pavement Design, **(22)**:sup1, S672-S689.

Saxena A, Kumar V.V., Correia NS, Zornberg, JG (2023) Evaluation of Millability and Recyclability of Asphalt with Paving Interlayers, Geotech. Testing Journal, **47(1)**: GTJ20230326.

Tran N, Julian G, Taylor A, Willis R, Hunt D (2012) Effect of geosynthetic material in reclaimed asphalt pavement on performance properties of asphalt mixtures. Transp. Res. Rec. **2294 (1)**: 26–33.

West RC (2015). Best Practices for RAP and RAS Management, Technical Report D, Lunham, MD, USA, 44p.

Zaumanis M, Loetscher D, Mazor S, Stockli F, Poulikakos L (2021) Impact of milling machine parameters on the properties of reclaimed asphalt pavement. Construction and Building Materials **(307):** 125114.

Accepted manuscript doi:
10.1680/jgein.24.00060

Tables

Table 1. Characteristics of the paving geosynthetics investigated in this study.

Properties	GS1	GS2	GS3	GS4	GS5
Geogrid composition	Fiberglass	Fiberglass	-	Fiberglass	Polyester
Fabric composition	-	Polypropylene	Fiberglass mesh/ polyester mat	Polypropylene	Polypropylene
Apperture size, mm	20x25 (aperture)	31x30	-	31x32	32x39
Coating type	polymeric	-	Elastomeric bitumen	bitumen	bitumen
Mass per unit area (ASTM D5261), g/m²	412.0	382.0	145.0	326.0	272.0
Mass per unit area of geotextile backing (ASTM D5261), g/m²	-	168.4	-	27.5	45.7
Thickness (ASTM D5199), mm	1.5	1.8	0.45	1.35	1.8
Thickness of geotextile backing (ASTM D5199), mm	-	1.35	-	0.13	0.21
Asphalt retention capacity of the geosynthetic (ASTM D6140),	422.8	1553.7	432.1	421.1	395.8

g/m^2					
Ultimate tensile strength MD/CMD* (ASTM D6637), kN/m	75/97	50/50	25/30	50/50	50/50
Strain at ultimate tensile strength (ASTM D6637), %	≤ 3.0	≤ 3.0	≤ 7.0	≤ 3.0	≤ 10.0

*MD=Machine direction; CMD=Cross machine direction.

Table 2. Milling efficiency of geosynthetic-reinforced asphalt layers.

Properties	Control	GS1	GS2	GS3	GS4	GS5
Geogrid composition	Fiberglass	Fiberglass	-	Fiberglass	Polyester	Geogrid composition
Fabric composition	-	Polypropylene	Fiberglass mesh/ polyester mat	Polypropylene	Polypropylene	Fabric composition
Milling time (s)	96.0	99	117	114	118	145
Moving speed of the milling machine (m/min)	6.25	6.06	5.13	5.26	5.08	4.14
Milling efficiency (%)	100%	97%	82%	84%	81%	66%

Table 3. Marshall Stability parameters of asphalt mix containing RAP and G-RAP.

Properties	Design specification (DNIT	Control	20% RAP-C	20% G-RAP 1	20% G-RAP 2	20% G-RAP 3	20% G-RAP 4	20% G-RAP 5

	031/2024)							
Asphalt content (%)	-	5.0	5.6	5.2	5.3	5.4	5.5	5.5
Voids in mineral aggregates (%)	>15	15.03	16.85	15.86	15.92	16.31	16.58	16.51
Voids filled with asphalt (%)	75 a 82	77.48	77.66	76.98	77.89	77.97	77.36	77.42
Air voids (%)	3 to 5	3.39	3.76	3.65	3.52	3.59	3.76	3.73
Stability (kN)	>5	17.1	12.0	14.1	13.1	13.0	12.8	13.8
Flow (mm)	2.5 to 4.5	2.4	3.04	2.87	3.18	3.8	3.34	3.43
Indirect tensile test (MPa)	>0.65	0.79	1.2	1.07	1.03	1.18	1.22	1.41

Accepted manuscript doi:
10.1680/jgein.24.00060

Figure captions

Figure 1. Field test sections at Salvador International Airport: (a) overall location of the sections; (b) layout of the geosynthetic-reinforced sections.

Figure 2. Asphalt surface preparation, showing details of: (a) milling machine; (b) milling process; (c) surface texture.

Figure 3. The tack coat application process: (a) emulsion application using a spray bar; (b) view of the tacked area ready for the overlay construction.

Figure 4. Geosynthetic interlayers used in this study: (a) GS1; (b) GS2; (c) GS3; (d) GS4; and (e) GS5.

Figure 5. Geosynthetic interlayers installed in the experimental test sections at Salvador International Airport.

Figure 6. Asphalt overlay construction: (a) asphalt sanding technique; (b) paving equipment; (c) compaction process; (c) view of the constructed test section indicating milling direction.

Figure 7. Details of the milling machine Wirtgen W1000L and picks used in this study.

Figure 8. Pavement cross-sections for the different phases of the milling study.

Figure 9. Milling process of geosynthetic-reinforced test sections: (a) view of milling operation; (b) geosynthetic location within the milled layer.

Figure 10. Milling process of sections with fiberglass products: (a) area after milling; (b) milling drum with no geosynthetic fragments; (c) large geosynthetic fragments being collected in a truck; (d) fragments of geogrid observed in G-RAP1; and (e) fragments of geotextile fragments observed in G-RAP2.

Accepted manuscript doi:
10.1680/jgein.24.00060

Figure 11. Milling process of the polymeric-reinforced asphalt section: (a) tangled geogrid in the milling drum; and (b) polymeric filaments observed.

Figure 12. G-RAP produced from milling geosynthetic-reinforced sections: (a) Disposal of millings; (b) G-RAP and RAP-C stockpiles; (c) Close up view of the different G-RAP samples.

Figure 13. Particle size distribution of the produced G-RAP samples in comparison with control RAP.

Figure 14. Presence of geosynthetic milled fragments and fibers in the produced G-RAP retained in sieve #200: (a) G-RAP1; (b) G-RAP2; (c) G-RAP3; (d) G-RAP4; (e) G-RAP5.

Accepted manuscript doi:
10.1680/jgein.24.00060

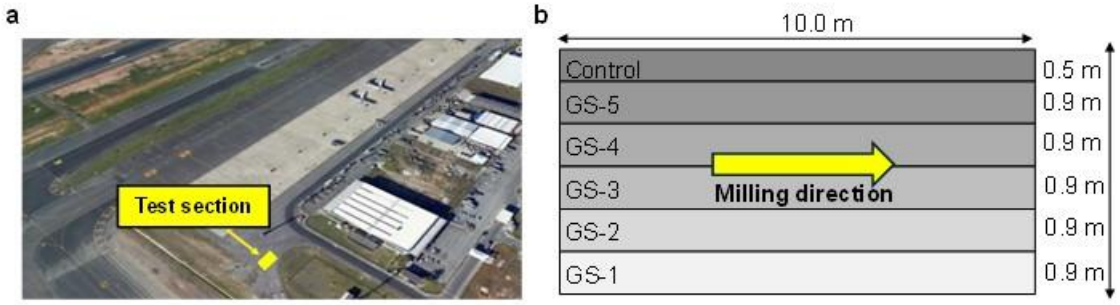

Fig. 1

Fig. 2

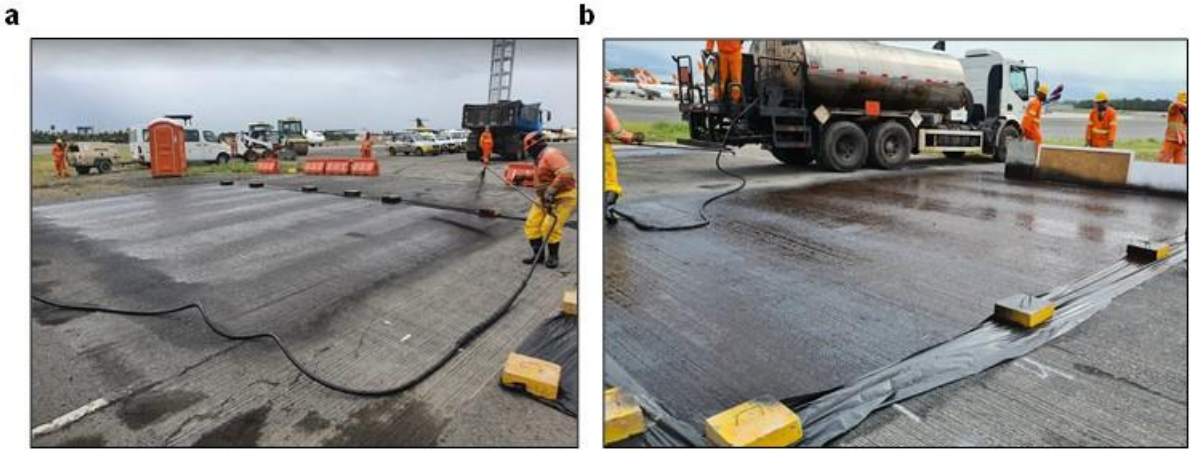

Fig. 3

Accepted manuscript doi:
10.1680/jgein.24.00060

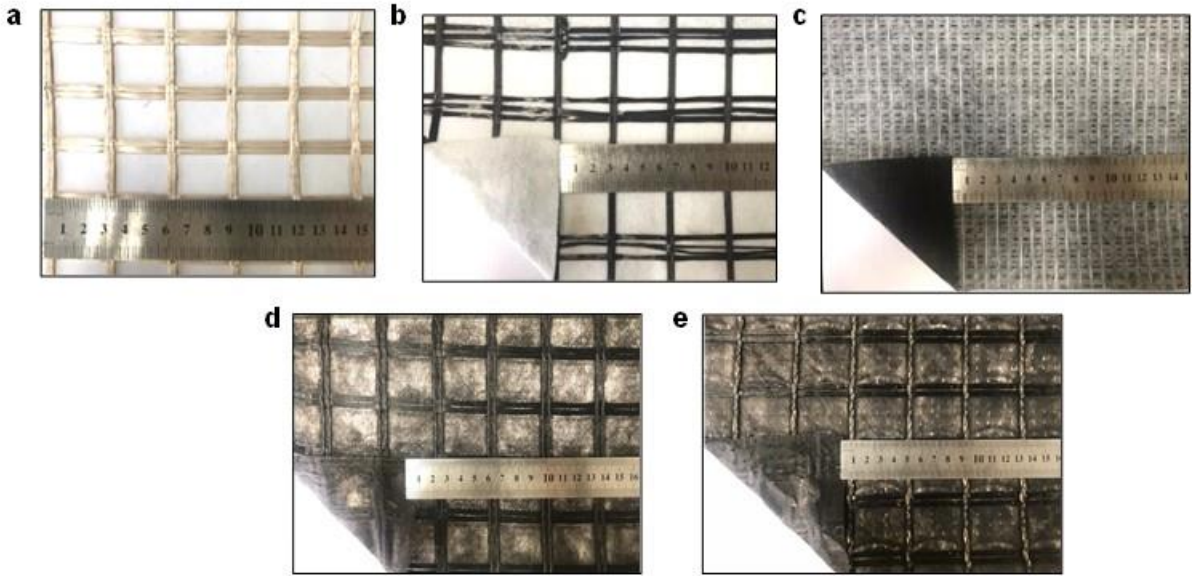

Fig. 4

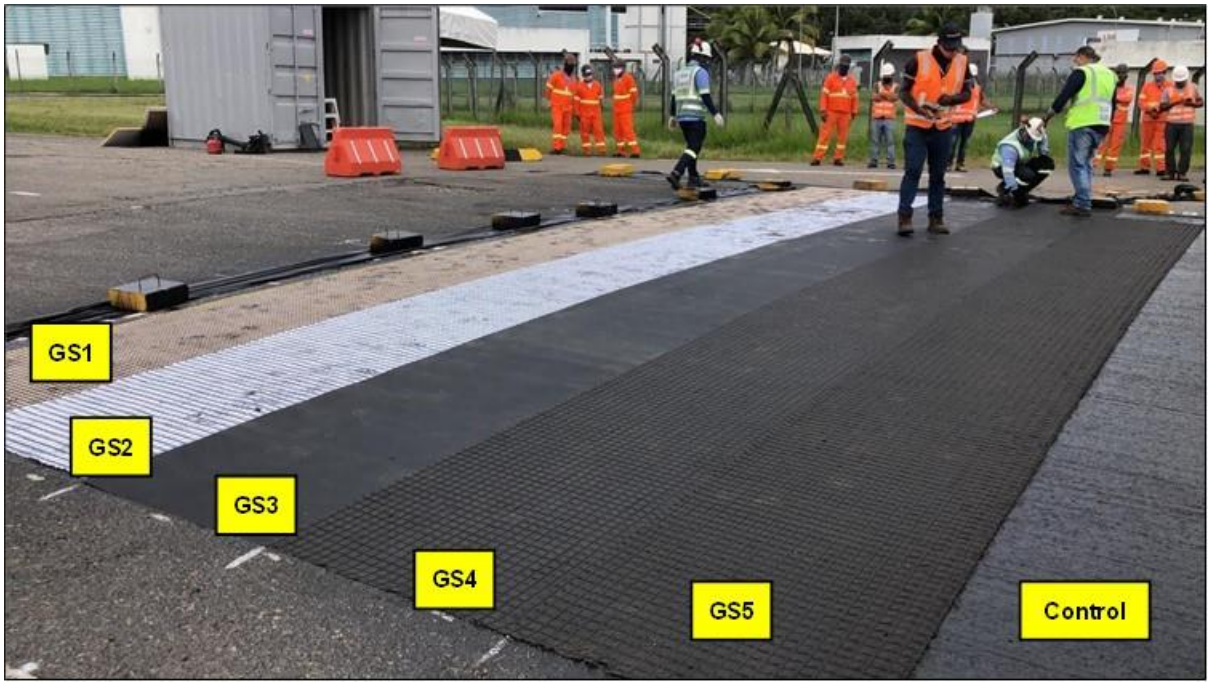

Fig. 5

Accepted manuscript doi:
10.1680/jgein.24.00060

Fig. 6

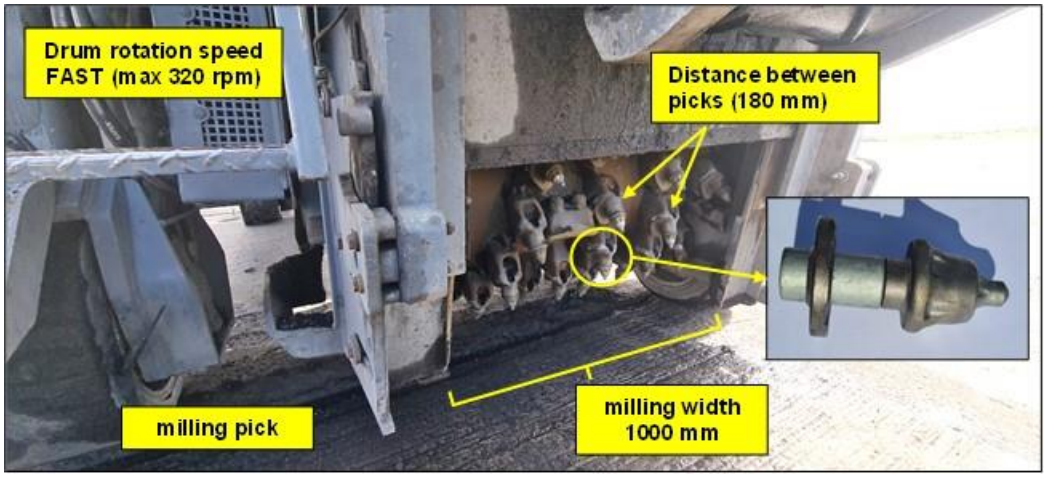

Fig. 7

Accepted manuscript doi:
10.1680/jgein.24.00060

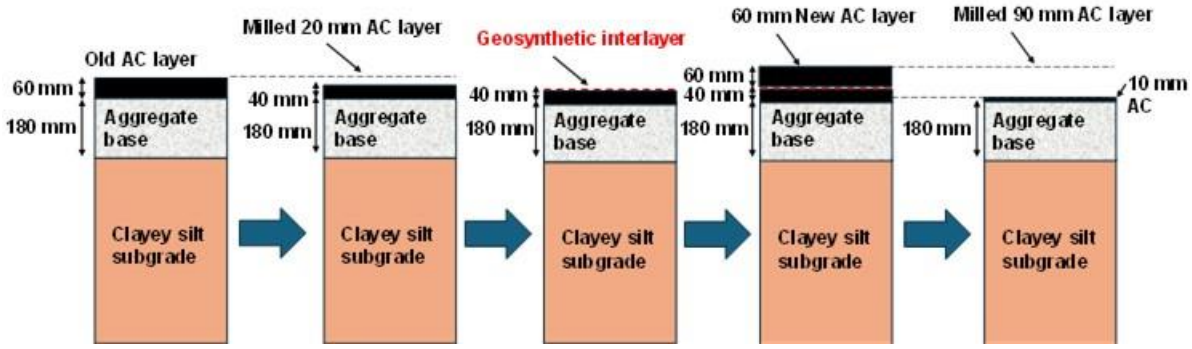

Fig. 8

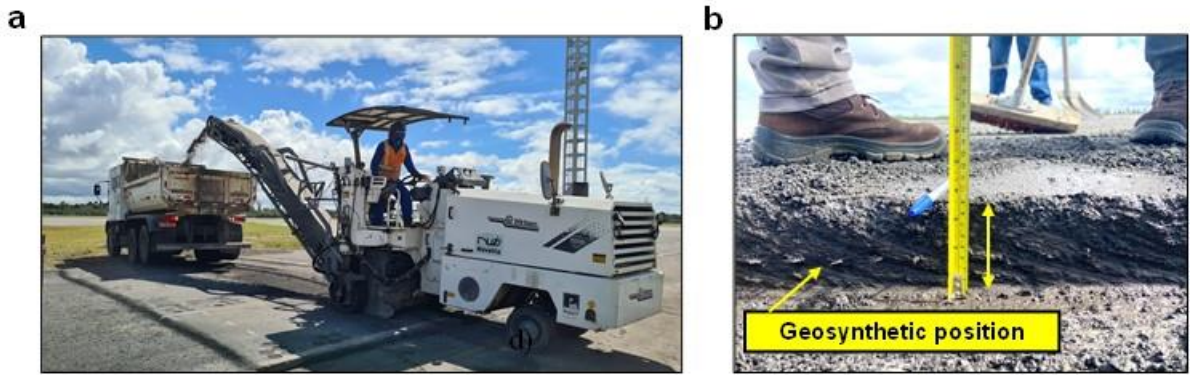

Fig. 9

Accepted manuscript doi:
10.1680/jgein.24.00060

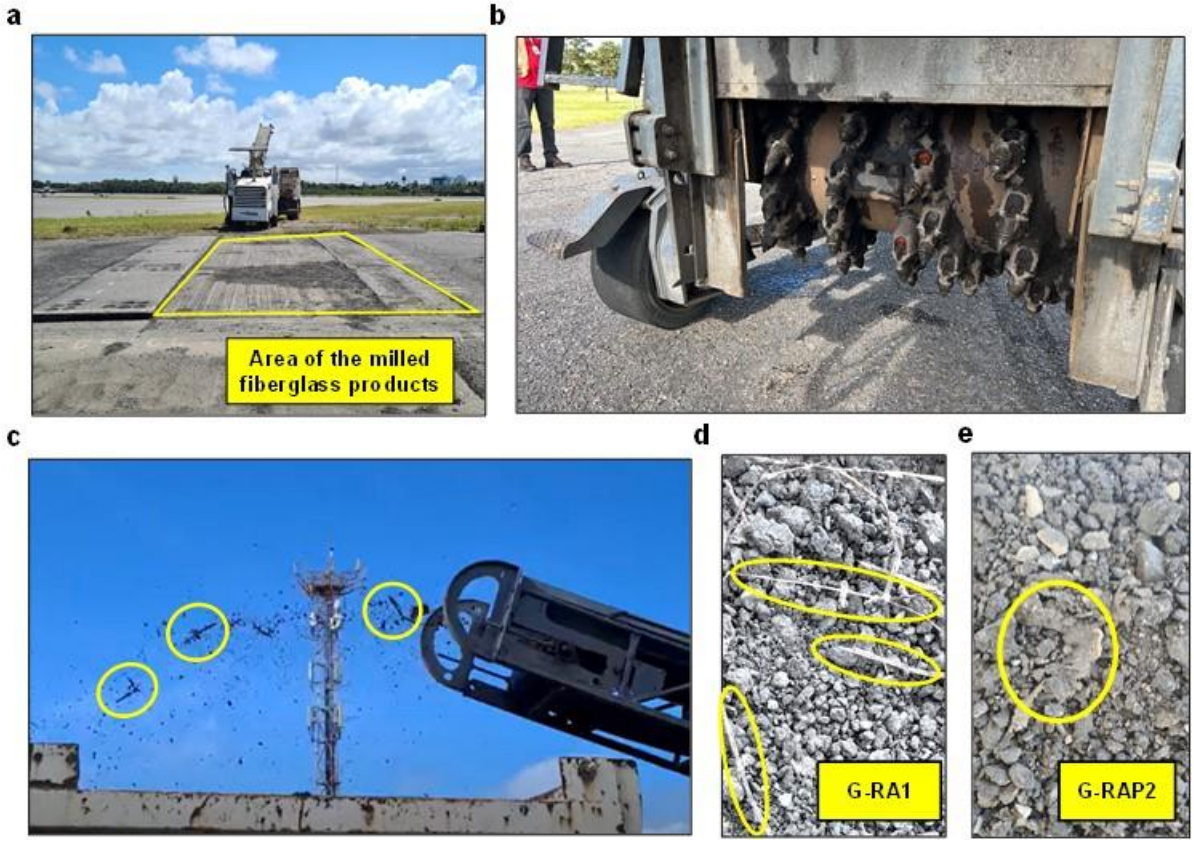

Fig. 10

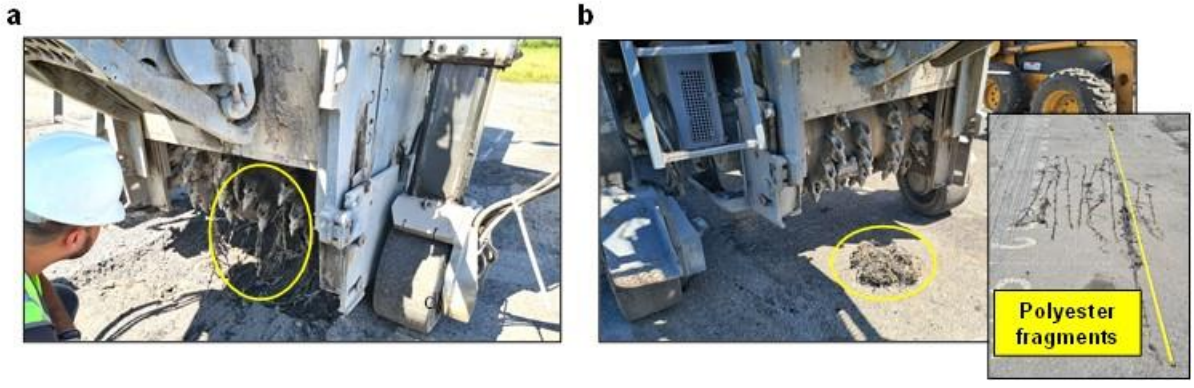

Fig. 11

Accepted manuscript doi:
10.1680/jgein.24.00060

Fig. 12

Accepted manuscript doi:
10.1680/jgein.24.00060

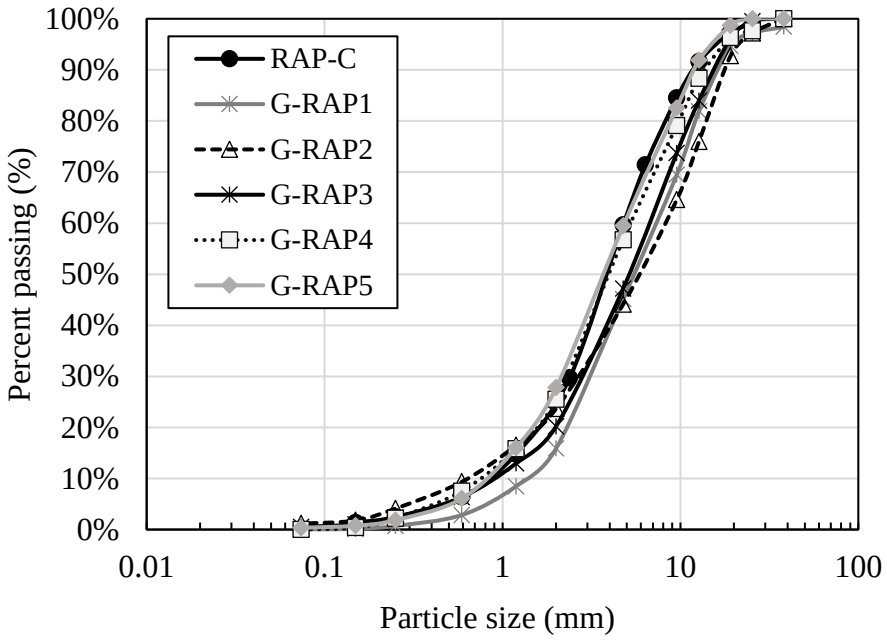

Fig. 13

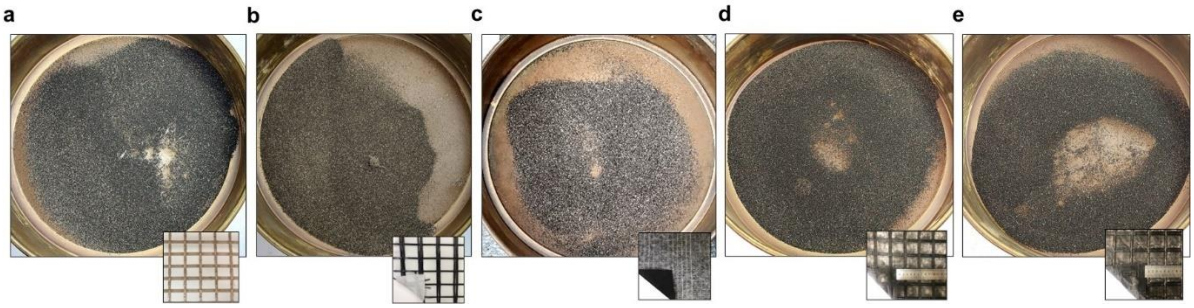

Fig. 14